Research Article

Open-Source Human Skin Model with an *In Vivo*-like Barrier for Drug Testing

Patrícia Zoio[1], Sara Lopes-Ventura[1], Joana Marto[2] and Abel Oliva[1,3]

[1]Instituto de Tecnologia Química e Biológica, Universidade Nova de Lisboa, Oeiras, Portugal; [2]Research Institute for Medicines (iMed.ULisboa), Universidade de Lisboa, Lisboa, Portugal; [3]Instituto de Biologia Experimental e Tecnológica (IBET), Oeiras, Portugal

Abstract

There is a global trend towards the development of physiologically relevant *in vitro* skin models to reduce or replace animal testing in the evaluation of therapeutic drug candidates. However, only commercial reconstructed human epidermis models (RHEm) have undergone formal validation. Although these commercial models are suitable for a wide range of applications, they are costly, lack flexibility, and the protocols used to generate them are not transparent. In this study, we present an open-source full-thickness skin model (FTSm) and assess its potential for drug testing. The FTSm was developed using endogenous extracellular matrix to recreate the dermal compartment, avoiding animal-derived hydrogels. An RHEm based on an open-source protocol was evaluated in parallel. The integrity of the skin barrier was analyzed by challenging the surface with detergents and measuring cell viability as well as by trans-epithelial electrical resistance (TEER) measurements. Skin irritation studies were performed based on OECD guidelines and complemented with an evaluation of the impact on the skin barrier by TEER measurement. The permeation of a dye through the developed models and a commercial membrane (Strat-M®) was compared using Franz diffusion cells and an infinite dose approach. The FTSm demonstrated structural and barrier properties comparable to native human skin. Although the RHEm showed a better performance in drug testing, the FTSm presented better barrier properties than commercial models as reported in the literature. These skin models can be a valuable contribution to accelerating the development and dissemination of alternatives to animal testing, avoiding the limitations of commercial models.

1 Introduction

Skin diseases are ranked as the fourth leading cause of non-fatal morbidity worldwide, affecting approximately one third of the global population (Seth et al., 2017). This is fueling the growth of the topical drug delivery market and leading to the development of new and better technologies (Tadros et al., 2020; Yamada and Prow, 2020; Cui et al., 2021). To investigate their mode of action and evaluate potential toxicity, animal models are extensively used in the preclinical phase of topical drug development (Almeida et al., 2017). However, they frequently lack predictive value for human skin conditions, resulting in high drug attrition rates at later stages of drug development (Van Norman, 2019). These factors, combined with the global legislation commitment to the development of new test methods in accordance with the 3Rs (replacement, reduction, and refinement of animal experimentation) and the European Union directives prohibiting the use of animal models for cosmetics, have increased the demand for non-animal alternatives to test topical formulations (Zuang et al., 2015; Gray et al., 2016).

In the last decade, major progress has been made in the development of physiologically relevant *in vitro* human skin models (Niehues et al., 2018). These models have been extensively used to evaluate the safety and efficacy of new drug formulations or cosmetic ingredients and to study skin biology and skin-related diseases. However, the complex multi-layered structure and physiology of the native human skin makes it challenging to develop reproducible models that accurately mimic its behavior (van den Broek et al., 2017).

From a histological point of view, the skin is composed of two main layers: the epidermis and the dermis, tightly connected by the dermo-epidermal junction (DEJ) (Joffe et al., 2020). The epi-

Received November 18, 2021; Accepted March 14, 2022;
Epub March 23, 2022; © The Authors, 2022.

ALTEX 39(3), 405-418. doi:10.14573/altex.2111182

Correspondence: Abel Gonzalez Oliva, PhD
Instituto de Tecnologia Química e Biológica (ITQB)
Universidade Nova de Lisboa
Avenika da República, Estação Agronómica Nacional
2780-157 Oeiras, Portugal
(oliva@itqb.unl.pt)

dermal layer is a stratified squamous epithelium containing mainly keratinocytes in close association with melanocytes. Keratinocytes form a proliferative basal layer and differentiate as they move towards the surface of the skin (Rice and Rompolas, 2020). This process gives rise to the different layers of the epidermis including the *stratum basale* (SB), *stratum spinosum* (SS), *stratum granulosum* (SG), and the most superficial portion, the *stratum corneum* (SC). This outer layer is formed by dead and denucleated keratinocytes (corneocytes), filled with keratin and surrounded by lipids, forming a water-resistant and protective barrier (Perticaroli et al., 2019). Melanocytes proliferate less frequently and remain at the DEJ where they interact with the basal layer, playing a crucial role in UV protection (Del Bino et al., 2018).

The dermis lies between the epidermis and subcutis and is mainly composed of human dermal fibroblasts embedded in a collagen matrix. Fibroblasts secrete and remodel extracellular matrix (ECM) components such as collagen and fibronectin, forming most of this connective tissue and providing a framework and mechanical support to the skin cells (Urciuolo et al., 2019). *In vivo*, the epidermis is bound tightly to the dermal component via the basement membrane, which is composed of ECM proteins secreted as a result of interactions between keratinocytes and fibroblasts. The DEJ facilitates the exchange of substances and the polarity of the basal keratinocytes (Natsuga et al., 2019).

Engineered skin models are incrementally advancing in emulating the anatomy of the skin. For reconstructed human epidermal models (RHEm), many researchers rely on commercially available *in vitro* skin models such as EpiSkin®, SkinEthic®, and EpiDerm® (Netzlaff et al., 2005). These models are generated by seeding keratinocytes on a polycarbonate membrane followed by establishment of an air-liquid interface to achieve epidermal differentiation. However, as they are based only on keratinocytes, they lack crosstalk with the dermis, which limits their application (Wang et al., 2016). More complex full-thickness skin models (FTSm) are also commercially available, namely Phenion®, Epiderm-FT®, Stratatest,® and T-Skin® (Ackermann et al., 2010; Rasmussen et al., 2010; De Wever et al., 2015a). These models are created using hydrogel-based technologies, usually with animal-derived collagen, into which fibroblasts are integrated. Although these structures mimicking the dermis provide good support to the epidermis and allow communication between keratinocytes and fibroblasts, they present several disadvantages. These include the use of exogenous animal-derived materials, fibroblast-mediated collagen contraction that results in detachment from the insert, low mechanical stability, and batch-to-batch variability (Redden and Doolin, 2003; Radhakrishnan et al., 2020).

All commercially available skin models have in common that the methods used to generate them are not fully transparent since they are partly based on confidential and legally protected protocols (De Wever et al., 2015b). Moreover, these models are costly and arrive pre-made, lacking the flexibility to be tailored for specific applications. Commercial models can also be affected by quality loss after shipment over long periods of time and distances. To surpass these restrictions, it is crucial to develop open-source protocols for the generation of reconstructed skin models. The open-source concept was first described in information technology (IT) with LINUX being the most popular example of a free and open software (Fuggetta, 2003). Reconstructed skin models based on this open concept could lead to independence from commercial suppliers and cost reduction for users. Recently, attempts have been made to develop *in vitro* skin irritation tests based on open-source RHEm with openly accessibly protocols (Mewes et al., 2016). A similar validation for open-source FTSm is still lacking.

In the present study, we tested the feasibility of using a previously developed open-source FTSm based on a fibroblast-derived matrix (FDM) and scaffold technology for drug testing applications (Zoio et al., 2021a). The developed model avoids the use of animal-derived hydrogels and the consequent problems arising from the use of animal collagen-based techniques. These characteristics make it ideal for applications where reproducibility and robustness are required, including integration on an organ-on-a-chip device (Zoio et al., 2022). We compare the physiology and overall performance of the open-source FTSm with an in-house RHEm produced using an open-source protocol (De Vuyst et al., 2013). The integrity of the epidermal barrier was assessed by challenging the surface of the epithelium and by performing transepithelial resistance (TEER) measurements. Irritation tests were performed according to OECD test guidelines (TG) and complemented with TEER measurements (OECD, 2021). Finally, permeation studies using Franz diffusion cells were performed on the open source FTSm and compared with the RHEm and the commercial membrane Strat-M®.

2 Materials and methods

2.1 Primary cells and cell maintenance

Primary human foreskin-derived dermal fibroblasts (HDFn; CellnTec, Bern, Switzerland) were maintained in fibroblast growth medium (FGM) composed of Iscove's Modified Dulbecco's Medium (IMDM, ThermoFisher, Loughborough, UK) supplemented with 10% fetal bovine serum at 37°C in a 5% CO_2 humidifier, following supplier's instructions. HDFs were used for up to 8 passages and subcultured at confluency between 80 and 90%.

Primary human epidermal keratinocytes isolated from neonatal foreskin (HEKn, ThermoFisher, Loughborough, UK) were maintained in keratinocyte growth medium (KGM) composed of EpiLife medium (ThermoFisher Scientific), supplemented with 0.06 mM calcium and keratinocyte growth factor (HKGS, ThermoFisher) at 37°C and 5% CO_2 in a humidified incubator. The KGM medium was changed every other day until the cells reached 50% confluency. At this point, the medium was changed every day until reaching 70-80% confluency. A low passage (3-4) and actively proliferating keratinocytes were used for successful 3D culture.

2.2 Generation of the open-source FTSm

The development of a FTSm based on a FDM comprises the development of a mature dermis composed of fibroblasts and ECM and the formation of a differentiated epidermis on top of the der-

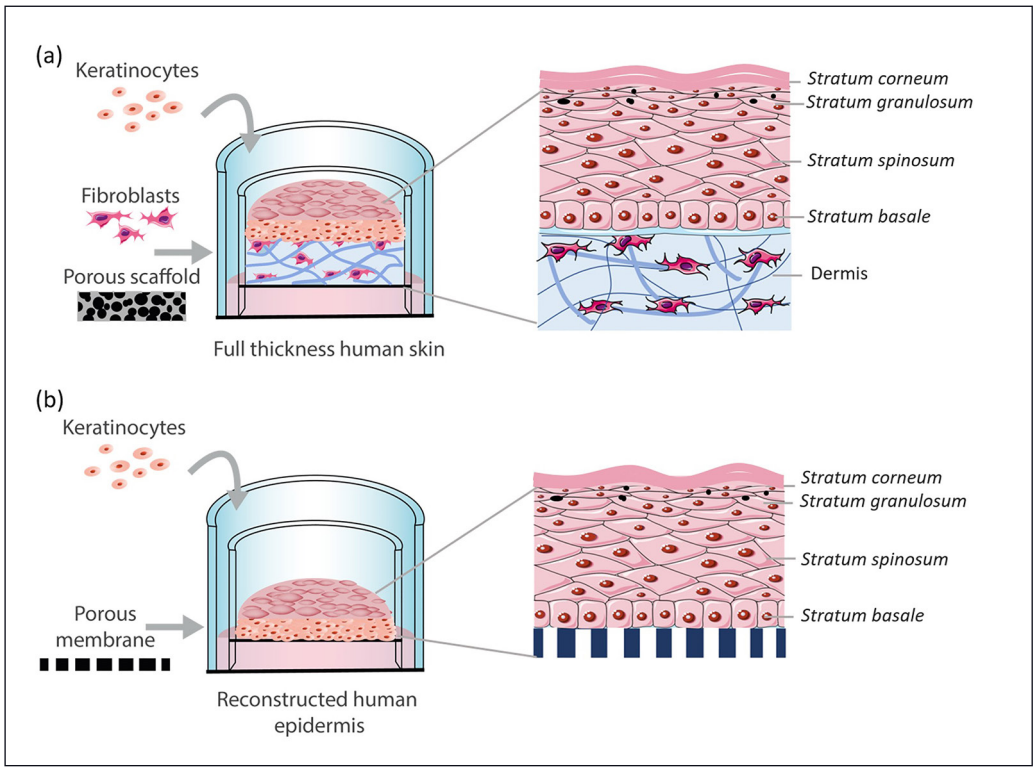

Fig. 1: Schematic depiction of the open-source (a) full-thickness model (FTSm) and (b) reconstructed human epidermis model (RHEm)
FTSm are generated using a porous polystyrene scaffold seeded with fibroblasts to recreate the dermal layer, and keratinocytes are seeded on top of the dermal layer. RHEm are generated by seeding keratinocytes on top of a porous membrane. An air-liquid interface is established to generate a fully-differentiated epidermis with the layers present in native human skin.

mis. The in-depth protocol has been previously published (Zoio et al., 2021a). Figure 1a shows a schematic representation of the FTSm with a scaffold structure and HDFns to generate the dermal compartment and the HEKns generating a stratified epidermal compartment.

Polystyrene scaffolds (12-well Alvetex® scaffold inserts, REPROCELL Europe Ltd, Glasgow, UK) were used for formation of the fully-human dermal equivalent. These scaffolds were selected due to their biological inertness, high porosity (90%) and low thickness (200 µm), and high pore interconnectivity. In the 12-well insert format, the scaffold has a diameter of 15 mm and an effective area of 1.12 cm^2. HDFns (1.0 x 10^6 cells) were seeded onto the porous scaffolds in 100 µL FGM medium (10 x 10^6 cells/mL) and incubated for 1.5 h at 37°C in a humified atmosphere with 5% CO_2. After the cell adhesion period, the scaffolds were placed with a sterile pair of tweezers in 6-well tissue culture plates (VWR). FGM supplemented with 100 µg/mL ascorbic acid 2-phosphate (Sigma-Aldrich) was applied to the bottom of each well to flood the insert prior to incubation and maintained for 9 days, changing the medium every 3 days. During this period, HDFns were stimulated to proliferate and secrete endogenous dermal ECM.

The FTSm were generated by seeding HEKn onto the dermal equivalents. As a first step, HEKns (5.0 x 10^5 cells) were incubated under submerged conditions in KGM containing a high concentration of calcium (1.5 mM). After 3 days, the models were raised to the air-liquid interface (ALI) by removal of the medium in the upper compartment and cultured in KGM containing 1.5 mM calcium supplemented with 10 ng/mL KGF and 100 µg/mL L-ascorbic acid 2-phosphate. The medium was changed every other day, and the FTSm were maintained for 12 days.

2.3 Generation of an open-source RHEm

RHEm were generated based on the protocol from De Vuyst et al. (2013) with minor adaptations. HEKns were seeded in porous polycarbonate cell culture inserts with 12 mm diameter, 0.6 cm^2 effective area, and 0.4 µm pore size (Merck Millipore, Beeston, UK). Figure 1b shows a schematic representation of an RHEm generated on top of a porous membrane. Briefly, HEKns were harvested by trypsinization, centrifuged, and 3.0 x 10^5 cells/mL were re-suspended in KGM containing 1.5 mM calcium. The polycarbonate culture inserts were placed in 6-well tissue culture plates (VWR) containing 2.5 mL medium, and 500 µL of keratinocyte suspension was added into the upper chamber of each insert. After 24 h at 37°C in a humidified 5% CO_2 incubator, the models were raised to ALI by aspiration of the culture medium in the upper compartment of the insert. The medium was replaced with 1.5 mL KGM supplemented with 1.5 mM calcium, 100 µg/mL ascorbic acid 2-phosphate, and 10 ng/mL KGF and renewed every other day. The epidermal models were maintained for 12 days.

2.4 Histological analysis

The reconstructed tissues were fixed immediately after being taken out of culture in 10% neutral buffered formalin (Sigma). The samples were embedded in paraffin to allow for transverse sectioning. Sections (5 µm thick) were deparaffinized and rehydrated for morphological evaluation by standard hematoxylin and eosin (H&E) staining.

2.5 Barrier function

Effective concentration at 50% viability

The barrier function was assessed by determining the concentration at which a benchmark chemical reduces tissue viability by 50% (IC_{50}) after a fixed exposure time. For this, a range of concentrations of sodium dodecyl sulphate (SDS) from 0 to 5 mg/mL was topically applied (70 µL for the RHEm and 150 µL for FTSm) for 18 h. After exposure, samples were washed in phosphate buffered saline (PBS) to remove medium containing phenol red.

For the FTSm, scaffold discs were removed from the support by unclipping the plastic base and placed in 12-well plates. 1 mL MTT (1 mg/mL 3-(4,5-dimethylthiazol-2-yl)-2,5-diphenyltetrazolium bromide in PBS, Sigma-Aldrich) was added to each well and incubated at 37°C in a 5% CO_2 incubator for 3 h. The MTT solution was replaced by 1 mL acidified isopropanol. The plates were covered with parafilm, protected from light, and left at room temperature (RT) on a rotating platform for 30 min at 100 rpm to ensure blue formazan product was fully solubilized.

For the RHEm, inserts were removed from the 6-well plates, washed with PBS, and transferred into the 24-well plates prefilled with 300 µL MTT solution (1 mg/mL). RHEs were incubated at 37°C in a 5% CO_2 incubator for 3 h. Then, the culture inserts were immersed in 2 mL/well of acidified isopropanol and left for 2 h at RT on a rotating platform (100 rpm).

After the extraction, samples of the formazan solution of each well were mixed and transferred in two aliquots of 200 µL each into 96-well plates. Absorbance was read at 570 nm using a plate reader. Relative MTT values were calculated with control cultures being set at 100%. Values were normalized to nontreated skin models.

Barrier integrity evaluation by passive dye diffusion

The barrier function of the skin models was further studied by assessing the penetration of the passive dye Lucifer yellow (Sigma) in combination with detergent treatment. Solutions of various SDS concentrations (0-0.5% w/v in PBS) were applied topically (70 µL epidermal models and 150 µL full thickness model). After 2 h incubation at 37°C, the models were washed three times with PBS, and 1 mg/mL Lucifer yellow was topically applied to the models for 30 min, followed by three washes with PBS. The tissues were fixed with a neutral buffered 10% formalin solution (Sigma) and embedded in paraffin. Tissue sections were rehydrated, and nuclei were stained with 1 µg/mL of 4,6-diamidino-2-phenylindole (DAPI, Invitrogen, Waltham, MA, USA). Slides were mounted with VECTASHIELD (Vector Laboratories, Burlingame, CA, USA). Images were obtained using the Nikon Eclipse TE2000-S fluorescence microscope (Nikon instruments, Melville, NY, USA) and analyzed with the ImageJ software.

Transepithelial electrical resistance

The barrier integrity of RHE and FTSm models was also evaluated by monitoring the TEER. Measurements were taken using an EVOM Epithelial Volt/Ohm Meter and a pair of Ag/AgCl probes (WPI Europe, Friedberg, Germany). For both FTSm and RHEm, measurements were performed after 12 days of cell culture at the ALI, before their fixation in formalin. TEER values were calculated according to the following equation:

$$TEER = \left(R_{sample} - R_{blank}\right) \times A \quad \text{(Eq. 1)}$$

where R_{sample} is the resistance value for the skin model, R_{blank} is the resistance value of an insert without cultured cells, and A is the effective culture area (1.12 cm^2 for FTSm and 0.63 cm^2 for RHEm). For RHEm, the KGM was replaced with 300 µL PBS in the apical compartment and 2 mL PBS in the basal compartment. For FTSm, for the time required to measure electrical resistance, the tissues were placed in adapted 6-well plates containing 2 mL PBS. The KGM was aspirated and replaced with 250 µL of PBS in the apical compartment. One electrode was submerged in the upper compartment and the other was submerged in the lower compartment. Measurements were performed for four different skin batches of FTSm and RHEm. Together with TEER values measured for skin batches used in previous studies, a lower threshold was determined as a quality control by correlating the measurements with observations of macroscopical skin defects in histological analysis. FTSm and RHEm with TEER values lower than the determined threshold were not used for further experiments.

2.6 Skin irritation test

Study design and test protocol

The irritation tests were performed according to OECD TG 439 (OECD, 2021). The reference substances were 5% aqueous potassium hydroxide (Sigma) and 1-bromohexane (Sigma), which are both classified as irritants (category 2 substance) according to the United Nations Globally Harmonized System of Classification and Labelling of Chemicals (UN GHS), and isopropanol (Sigma) and diethylene glycol monoethyl (Transcutol®, Sigma), which are both classified as non-irritants (no category substance). Two controls were included in each test run. PBS was applied to the top of the models as a negative control (non-irritant), and 5% aqueous SDS served as positive control (irritating). Each chemical substance was tested in triplicate, and controls were tested in duplicate. All test compounds were pre-checked prior to use for direct MTT reduction and color interference as described in OECD TG 439.

Figure 2 shows the steps performed for skin irritation testing. The testing was performed according to DB-ALM Protocol nº 212 (epiCS SIT) with minor adaptations. Briefly, RHEm and FTSm were topically treated with the test substances (50 µL/cm^2) for 20 min. Following exposure, tissues were washed with PBS and incubated for 42 h at 37°C in a CO_2 incubator. The medium was exchanged 24 h after the application of the test samples. At the end of the post-incubation period, tissue viability was evaluated by MTT assay using the protocol described in Section 2.5. The reduction of cell viability in tissues treated with test substances was compared to tissues treated with negative control (100% viability) and expressed as % according to Equation 2:

$$\%Viability = \frac{OD_{sample}}{OD_{negative\ control}} \times 100 \quad \text{(Eq. 2)}$$

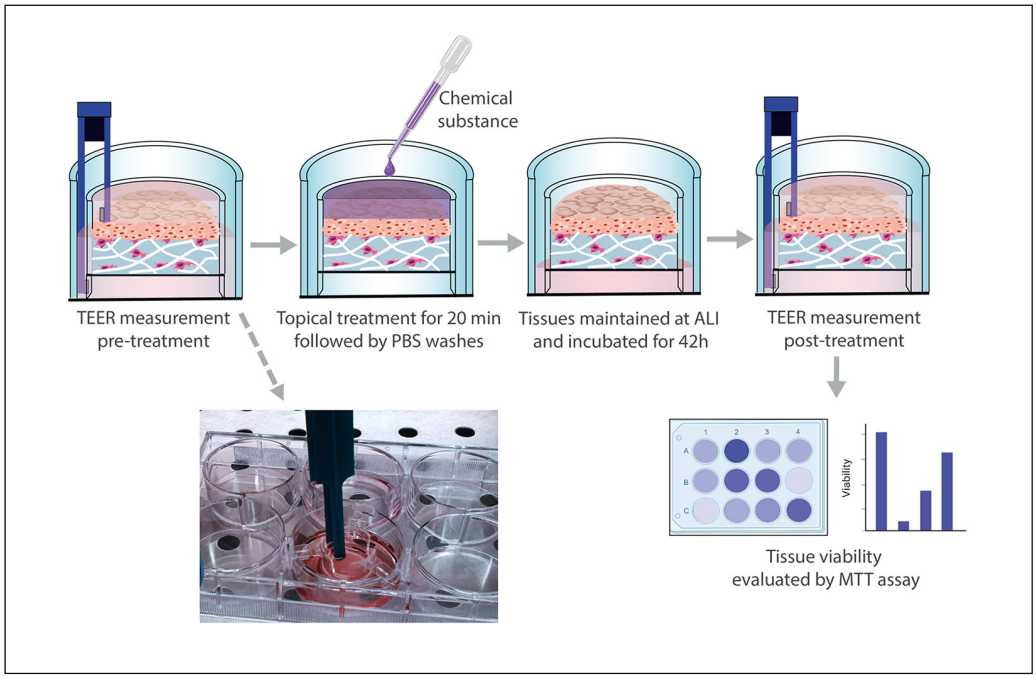

Fig. 2: Schematic of the protocol for skin irritation testing
TEER measurements were performed before application of the test substances using chopstick electrodes. Models were topically treated for 20 min followed by washes with PBS. The skin tissues were then incubated for 42 h at 37°C in a CO_2 incubator. After this incubation period, TEER measurements were performed, and the tissue viability was evaluated by an MTT assay.

Prediction/evaluation model

The prediction/evaluation model to assess chemical hazard based on OECD TG 439 uses a viability threshold to classify a substance (OECD, 2021). A substance was classified as "irritating" or "category 2" when the average viability after the skin irritation test obtained using the MTT assay was below or equal to 50%. A substance was classified "non-irritating" or "no category" when the mean viability was above 50%. Also, a tissue was considered as conforming if the mean OD values of the negative control were between 0.6 and 2.8 for every exposure time, which is the range that includes all OECD validated models, the mean viability of the tissue replicates exposed for 1 h with the positive control were < 15%, and the standard deviation (SD) was ≤ 18.

TEER for skin irritation test

TEER measurements were also performed as a complement of the skin irritation test. To evaluate the effects of chemical substances on the TEER values of fully matured RHEs and FTSm (day 12 of ALI), measurements were taken before and 42 h after exposing the tissue to the test substances. TEER measurements were performed as described in Section 2.5. Raw data of the TEER value for tissue were reported for the test substances in 3 replicates. The means and SDs of TEER values of selected compounds were normalized to untreated skin and reported as fold change over control.

2.7 Permeation assays using Franz diffusion cells

In vitro permeation tests were performed in static Franz cells (volume 4 mL, diffusion area of 1 cm^2) using the RHEm, FTSm, and Strat-M® (Merck Millipore, Tullagreen, Carrigtwohill, Ireland). Three test compounds with varying polarity were used for the permeation testing: clotrimazole (FIS – Fabbrica Italiana Sintetici S.p.A., Montecchio Maggiore, Italy) and hydrocortisone (Tianjin Jinjin Pharmaceutical Co., Ltd., Tianjin, China), both applied as a 1% (w/v) solution in propylene, and salicylic acid (Quimidroga, Barcelona, Spain), applied as a 1% (w/v) solution in propylene glycol/water 9:1. The experiments were performed in triplicate (n = 3) for FTSm, RHEm, and Strat-M® membranes. The RHEm and FTSm were visually inspected for any defects. Since both FTSm and RHEm were too small to be directly mounted into the Franz diffusion cells, dedicated adaptor modules were designed in AutoCad (Autodesk, Inc.) and fabricated using 3D-printing (Fig. S1, S2[1]). The adaptors allowed correct placement and sealing of the skin models in the center of the Franz cells (Fig. S3[1]).

The release medium was continuously stirred with a magnetic bar and maintained at 32 ± 2°C by a thermostatic water pump to assure a temperature of 32°C at the membrane surface (to mimic skin conditions). The receptor medium, a mixture of PBS:ethanol 3:1, was appropriately screened based on solubility studies to ensure the sink conditions during the experiment. Aliquots of the receptor phase (200 µL) were withdrawn after 1, 2, 4, 5, 6, 8 and 24 h and analyzed via UV at 298 nm for salicylic acid, 263 nm for clotrimazole and 254 nm for hydrocortisone.

The cumulative amount of drug that had permeated through the different models was plotted as a function of time (Q_t) and determined based on the Equation 3:

$$Q_t = \frac{V_r \times C_t + \sum_{t=0}^{t-1} V_s \times C_i}{S} \quad \text{(Eq. 3)}$$

[1] doi:10.14573/altex.2111182s

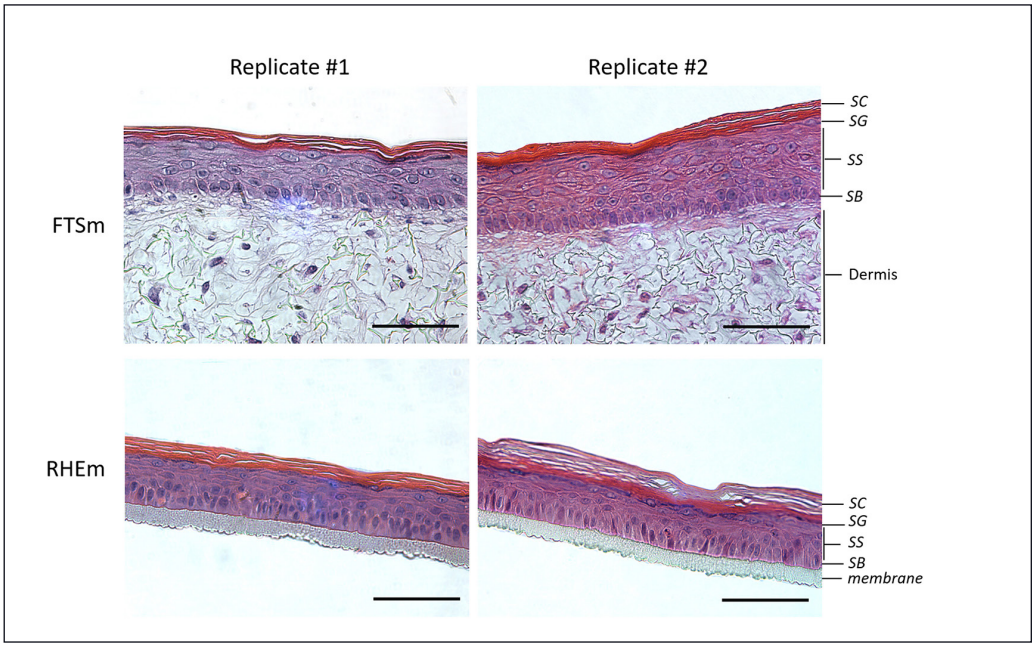

Fig. 3: Representative H&E images of two independent replicates of a full thickness skin model (FTSm) composed of dermal and epidermal compartment and a reconstructed human epidermal model (RHEm) Both models were maintained at the air-liquid interface for 12 days to promote epidermal differentiation. *Stratum corneum* (SC), *stratum granulosum* (SG), *stratum spinosum* (SS), and *stratum basale* (SB). Scale bars: 100 µm.

where C_t is the drug concentration of the receiver solution at each sampling time, C_i is the drug concentration of the sample applied on the donor compartment, and V_r and V_s are the volumes of the receiver solution and the sample, respectively. S represents the skin surface area.

According to Fick's first law of diffusion, the steady-state flux (J_{ss}, µg/cm^2/h) was calculated:

$$J_{ss} = D \times C_0 \times P/h = C_0 \times K_p \quad \text{(Eq. 4)}$$

where D is the diffusion coefficient of the drug, C_0 represents the drug concentration in the donor compartment, P is the partition coefficient between the vehicle and the skin, h is the diffusional path length, and K_p is the permeability coefficient.

The flux and K_p of the formulations were measured and compared accordingly. The J_{ss} and K_p of the yielded solutions were calculated and compared. The permeation lag time, a parameter related to the required time to achieve the steady-state flux of a drug through the skin, was also considered for analysis.

2.8 Statistical analysis

Data are presented as mean ± SD. Quantitative differences between samples and the viability threshold were assessed by one-way ANOVA; *, $p < 0.05$; **, $p < 0.01$; ***, $p < 0.001$.

3 Results

3.1 Open-source skin models recapitulate the morphology of human skin

The FTSm and RHEm were developed based on open source methodology and first described in Zoio et al. (2021a). The basic morphology of the generated models was analyzed by conducting H&E staining on transverse sections. Figure 3 shows that both skin models formed a complex architecture with a multi-layered epidermis after 12 days of culture at ALI. The models replicated the normal process of epidermal stratification, presenting the four main layers: SB, SS, SG and SC. As expected, in the lower part of the epidermis (SB), HEKns show a cuboid morphology, followed by the cells of the SS and SG with a flatter architecture, and anucleated cells closer to the surface. At the apical surface, a cornified layer can be seen in both models.

The FTSm includes a fully human dermis capable of supporting the multi-layered epidermis without HEKn infiltration. Figure 3 (top) shows the dermis compartment with HDFns distributed along the scaffold and FDM, which built up and accumulated in the pores, mimicking the composition of native human dermis.

3.2 Reconstructed full thickness skin models show improved barrier function

The barrier function of the RHEm and FTSm was assessed by testing the ability of the SC and its lipid composition to resist the rapid penetration of a cytotoxic benchmark (SDS) as estimated by IC_{50}. The viability of the models cultured at ALI for 12 days was assessed by MTT colorimetric assay. Upon application of various SDS concentrations, IC_{50} values of 1.5 mg/mL and 1.8 mg/mL were determined for RHEm and FTSm, respectively (Fig. 4a). These values were within OECD acceptance limits. Moreover, the tissue damage caused and the resultant disruption of the skin barrier were visualized by topical application of increasing concentrations of SDS (0.15 to 0.5%) for 2 h followed by observation of the passive diffusion of the hydrophilic fluorescent dye Lucifer yellow into FTSm (Fig. 4b) and RHEm (Fig. 4c).

When the dye was applied to an untreated skin model, it was retained in the SC, and no diffusion was observed into the epidermis or into the dermal layer, showing the integrity of the skin barrier for this molecule. In the skin models treated with SDS, the diffusion of the dye was dose-dependent, with the dye being mostly re-

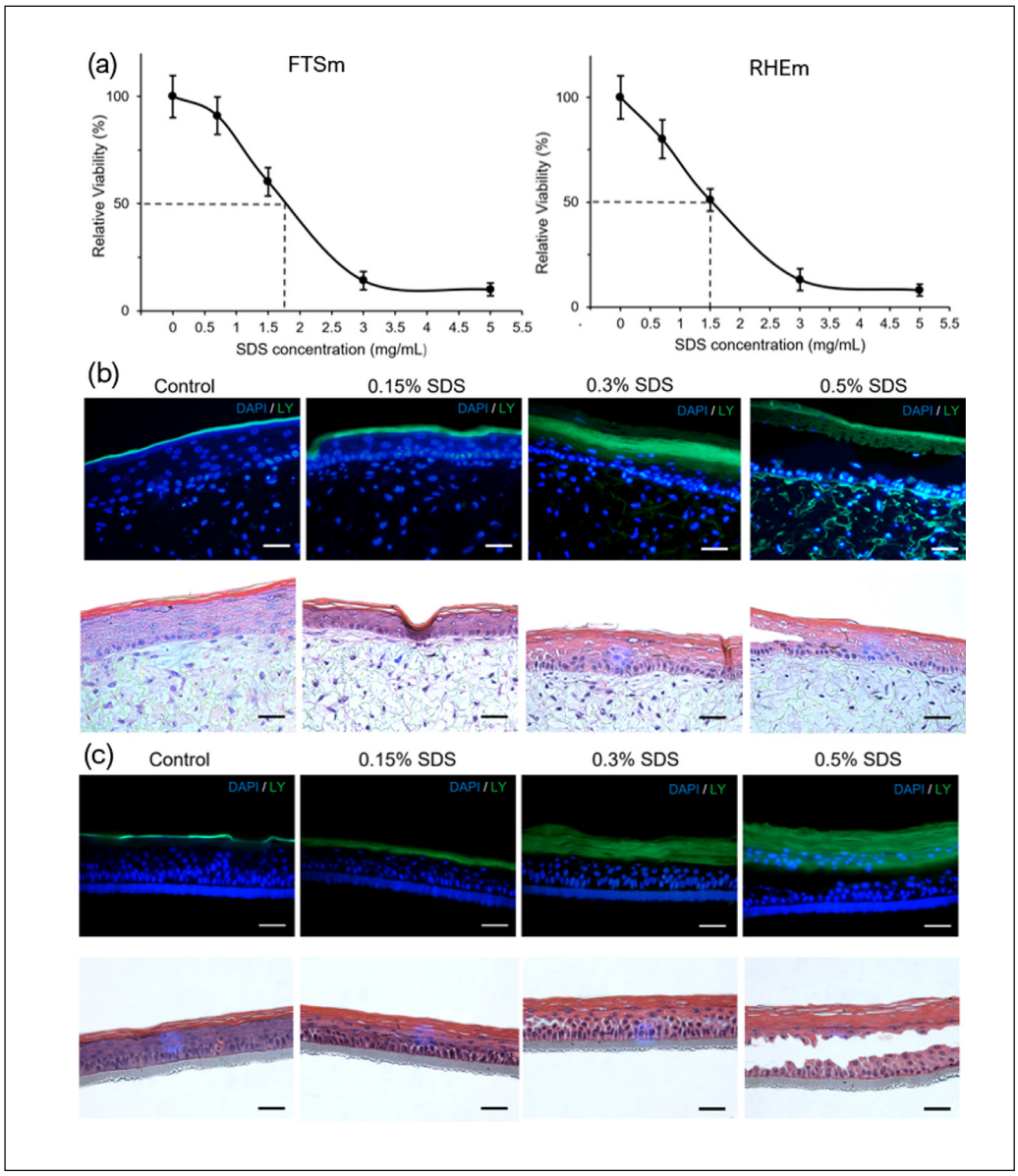

Fig. 4: Assessment of barrier properties in epidermal and full thickness models
(a) Analysis of metabolic activity (MTT conversion) in the epidermal model cultured for 10 days at the air-liquid interface before being exposed for 18 h to a concentration range of SDS to determine an IC_{50} value. Assessment of barrier resistance in (b) full thickness models and (c) reconstructed skin models. Representative fluorescence (top) and H&E images (bottom) of full thickness skin models and epidermal models cultured for 12 days at ALI. Samples were exposed to a concentration range of SDS for 2 h followed by the application of Lucifer yellow (LY) for 30 min to assess the penetration of the dye and barrier integrity. Nuclei are stained with DAPI (blue). Scale bar = 50 μm. The experiments were performed in triplicate (n = 3).

tained in the *stratum corneum* at lower SDS concentrations and penetrating further at higher SDS concentrations (> 3 mg/mL). A complete loss of epidermal integrity and barrier function was observed for skin models treated with 0.5% SDS.

To further assess the integrity of the cultures, TEER measurements were performed. This technique is useful to study the integrity of tight junctions and detect any barrier dysfunction. TEER was measured after cell culture for 12 days at ALI in both models. Considering 4 batches/biological replicates (N = 4) with different numbers of technical replicates each (n = 8,4,4,9) as well as our historical TEER values, FTSm presented mean TEER values of 953 ± 398 Ω.cm^2 (Fig. 5a), and RHEm presented mean TEER values of 11,424 ± 6,033 Ω.cm^2 (Fig. 5b).

For FTSm, a lower limit of 500 Ω.cm^2 was set as a quality control based on macroscopic evaluation of the skin models and through histological analysis. Models with lower TEER values presented macroscopic defects. An example of an extreme macroscopic defect can be seen in Figure S4[1]. A more common observation was the presence of small holes on the surface of the model where no epidermal compartment was present; however, no signs of keratinocyte infiltration were found. This problem, which affected 15% of the product FTSm, may be caused by irregularities in the scaffold structure, showing a need for protocol optimization. Only 3% of the produced FTSm presented lower TEER values caused by an undifferentiated epidermis. FTSm with TEER < 500 Ω.cm^2 were not used in further experiments.

For RHEm, a lower limit of 1500 Ω.cm^2 for TEER values was established as a quality control. In models with lower values, it was not possible to establish an ALI, and the inserts remained submerged. As expected, histological evaluation of these submerged models showed an undifferentiated structure. RHEm with TEER < 1500 Ω.cm^2 were not used in further experiments.

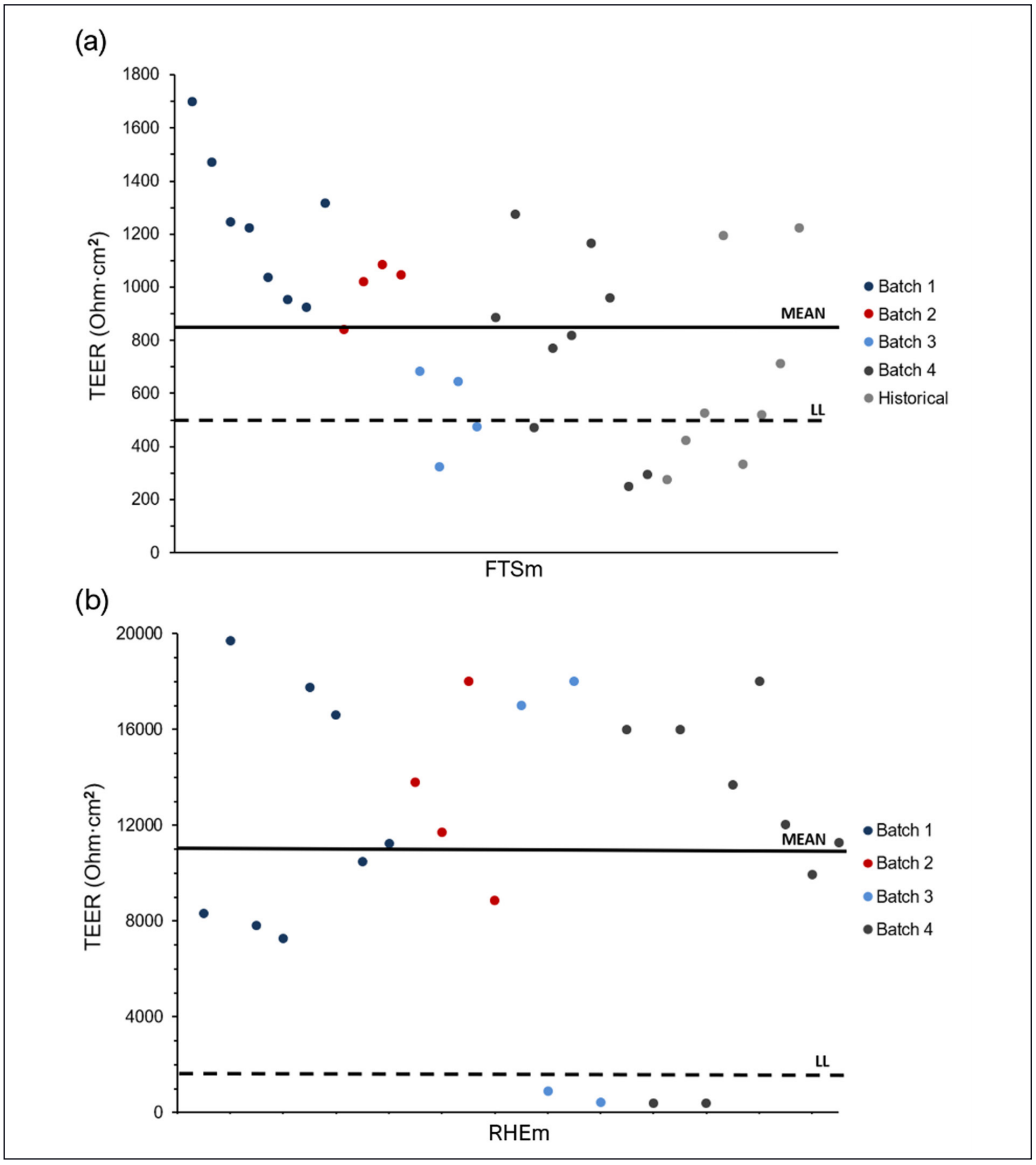

Fig. 5: Transepithelial electrical resistance (TEER) measurements performed with an EVOM system and chopstick electrodes obtained after 12 days of culture at the ALI, before fixing tissues in formalin, for (a) full thickness model (FTSm) and (b) reconstructed skin model (RHEm)
Data represent the different technical replicates for each batch and historical values. TEER is reported as $\Omega \cdot cm^2$ tissue surface area. The solid line represents the mean value, and the dashed line represents the defined lower limit (LL). EVOM, Epithelial Volt/Ohm Meter; TEER, transepithelial electrical resistance.

The different magnitude of mean TEER values of FTSm and RHEm does not correlate with differences in skin differentiation or barrier integrity. It can be hypothesized that the generally lower TEER measurements obtained for FTSm are a result of the specific insert geometry and sealing properties. The insert does not tightly seal the periphery of the scaffold. Therefore, leakage of PBS across the sealing area is not fully prevented and results in lower TEER values (Fig. S5[1]).

The scaffold structure avoided the contraction typically seen with collagen-based scaffolds. Figure S5[1] shows the FTSm after 12 days at ALI, without signs of contraction.

3.3 Open-source skin models are suitable to test irritation potential of substances

To evaluate the performance of the developed FTSm and RHEm for skin irritation tests, the effect of different chemical substances on cell viability and impedance was evaluated. A negative (PBS) and positive control (5% SDS solution) were included in every test run. Three substances suggested in OECD TG 439 were included (5% potassium hydroxide, isopropanol and 1-bromohexane) as well as one substance commonly used as a skin penetration enhancer in pharmaceuticals and cosmetic products (diethylene glycol monoethyl ether, Transcutol®).

After topical application of the chemical substances and subsequent post-incubation, cell viability was assessed using the MTT assay. The relative cell viability was normalized to the PBS-only treated tissues, and the relative values of FTSm were compared with values of RHEm (Fig. 6a). The OD values of the negative controls were 1.73 ± 0.27 for FTSm and 0.89 ± 0.03 for RHEm, meeting the acceptance criterion of $0.6 \leq OD \leq 2.8$. The positive control demonstrates the sensitivity of the tissue model to a known irritant. The mean viability of the positive control (relative to negative control) varied between 0.5% and 3%, meeting the acceptance criterion of < 15%. The SD for both models was

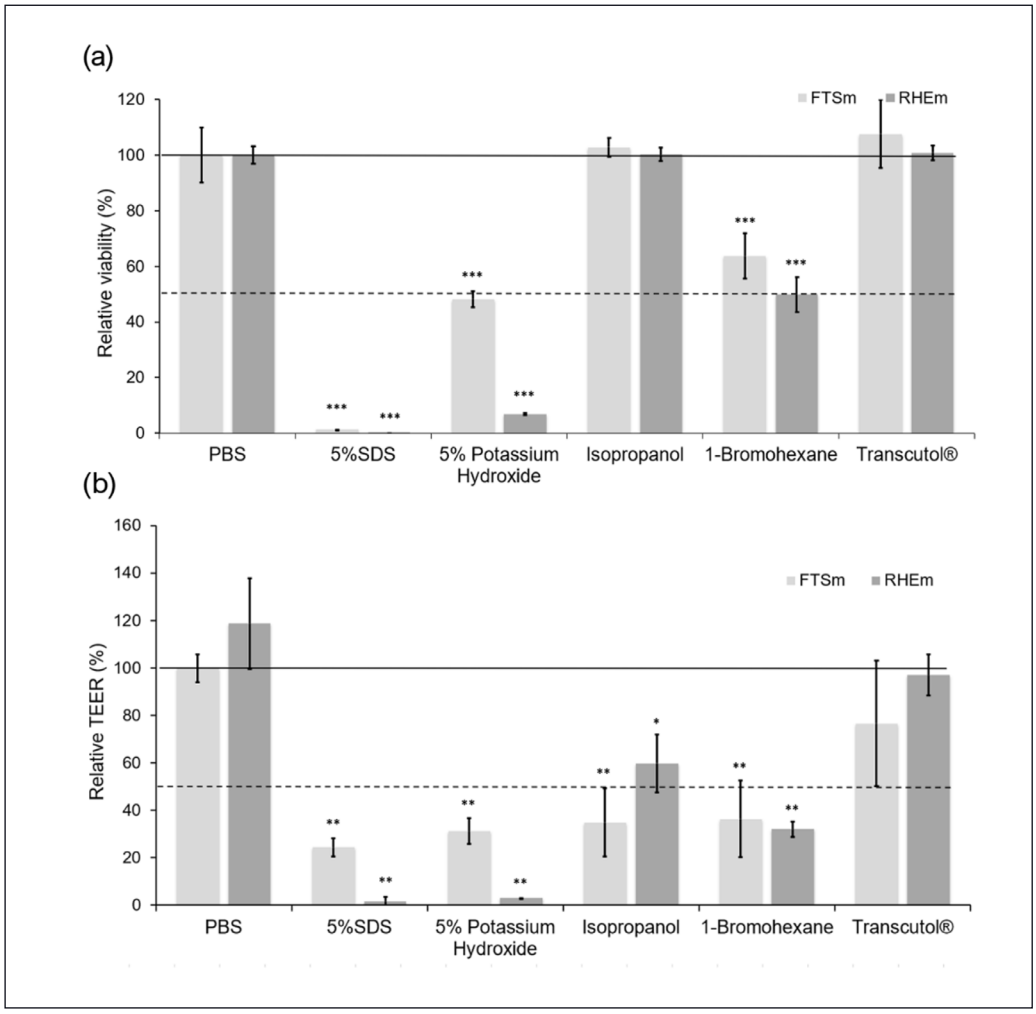

Fig. 6: Effect of the test substances on the skin models (FTSm and RHEm)
(a) Irritation tests evaluated by MTT analysis. The relative increase/decrease in viability was normalized to the change (in %) over the negative control (PBS, set to 100%, black solid line); 5% SDS was used as a positive control. The black dashed line shows the threshold of 50% viability compared to the negative control. (b) Irritation tests evaluated by TEER measurements. The relative increases/decreases in TEER values after treatment with test substance were normalized to the change (in %) over the TEER values before treatment (set to 100%, black solid line). The black dashed line shows the threshold of 50% compared to the TEER values before treatment with test substance. Data is expressed as mean ± SD from triplicate experiments.

always ≤ 18%. To identify the predictive capacity of the models, the *in vitro* classification obtained was compared to the reference *in vivo* classifications (OECD, 2021). MTT staining confirmed the irritative characteristics of 5% potassium hydroxide for both RHEm and FTSm. However, 1-bromohexane was only correctly identified by the RHE model (48% relative viability). Treatment of the FTSm with this substance resulted in a relative viability of 63.7%, which would lead to a classification as non-irritant (or category 2). Isopropanol and diethylene glycol monoethyl ether were correctly identified as non-irritants (no category) in both models.

In addition to viability, TEER was measured for RHEm and FTSm before application of the test formulations and before the MTT assay was performed (Fig. 6b). For both models, the application of the irritants 5% SDS, 5% potassium hydroxide and 1-bromohexane resulted in a marked decrease in TEER values. This effect was more pronounced in the case of RHEm. However, in both models, treatment with the irritants resulted in a reduction of at least 50% compared to TEER values before their application. Although the viability measurements correctly identified isopropanol as a non-irritant, treatment of FTSm with this substance reduced TEER values in a range that was comparable to the SDS group (70% reduction). For RHEm, the reduction in TEER values after treatment with isopropanol was less pronounced but showed a significant decrease of approximately 40% in the TEER values. For RHEm, when testing diethylene glycol monoethyl ether, no significant changes were detected in TEER, which correlates with the data from cell viability. For FTSm, the substance resulted in a 25 ± 25% decrease in TEER values.

3.4 Comparative permeation between the reconstructed skin models and artificial membranes

In the permeation assays, FTSm, RHEm, and Strat-M® membranes were mounted in Franz diffusion cells. The permeability coefficient of topically applied substances (both drugs and vehicle components) is highly dependent on their physicochemical characteristics such as lipophilicity (Cross et al., 2003). Considering this, permeation studies were performed for three standard compounds (salicylic acid, hydrocortisone and clotrimazole) with different polarities (n-octanol-water partition coefficient (log P) of 1.98, 1.61 and 5.84, respectively). The cumulative amounts of permeated drugs in the models and the steady-state flux were obtained.

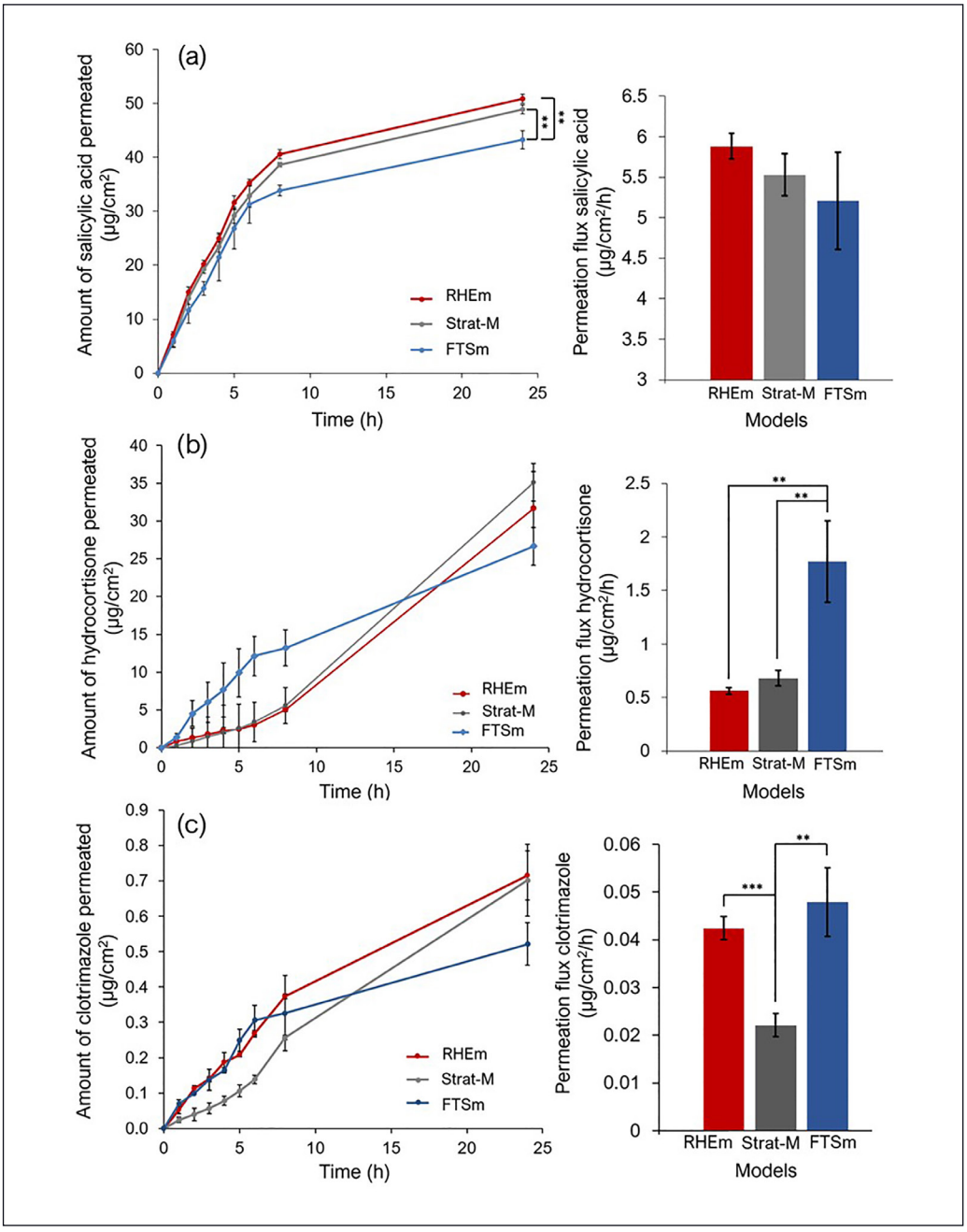

Fig. 7: *In vitro* permeation tests performed for a) salicylic acid, b) hydrocortisone, and c) clotrimazole
Experiments performed in static Franz diffusion cells using the RHEm, FTSm and Strat-M®. Cumulative amount of permeated (mean ± SD) (left) and steady-state flux (mean values ± SD) (right). The experiments were performed in triplicate (n = 3).

The steady-state fluxes calculated for salicylic acid using both RHEm and FTSm were not significantly different from the Strat-M® (Fig. 7a). However, the cumulative amount of permeated salicylic acid at 24 h was significantly lower using the FTSm. For hydrocortisone, high permeation fluxes through the FTSm were observed, compared to Strat-M® and RHEm (Fig. 7b). RHEm shows a 15% lower permeation rate than the Strat-M membranes. However, the amount of permeated hydrocortisone after 24 h was not significantly different between the skin models and Strat-M. For the experiment with hydrocortisone, FTSm show high standard deviations. The permeation flux of clotrimazole in both FTSm and RHEm was approximately double the flux compared to that through Strat-M® membranes (Fig. 7c). Again, the cumulative amount of clotrimazole at 24 h was not significantly different between the models.

4 Discussion

In this work, we studied the potential applications of an open-source FTSm with an *in vivo*-like architecture and optimized co-culture of fibroblasts and keratinocytes. The in-depth protocol to produce the FTSm was previously published by our group (Zoio et al., 2021a). This protocol uses an inert porous polysty-

rene scaffold as a support for the dermal compartment. Fibroblasts are seeded onto the scaffold and stimulated to secrete endogenous extracellular matrix, thereby avoiding the use of animal-derived collagen matrices. In the previous publication, we showed that this model, contrary to many conventional commercial models, presents good mechanical stability and is compatible with long-term cultivation. Furthermore, melanocytes can be added to recreate *in vivo*-like pigmentation. Here, multiple batches of FTSm with a fully differentiated epidermis were generated. The produced skin models mimicked the structure and function of native skin and recreated the layers characteristic of the native epidermis (SC, SG, SS, SP) on top of the mature dermis. An open source RHEm was also developed and evaluated in parallel. The feasibility of using the developed skin models for skin irritation testing was assessed by applying multiple chemical substances, following OECD guidelines, and performing skin permeation tests. The suitability of using TEER measurements as a non-destructive technique to quantify the barrier integrity of FTSm and RHEm was evaluated. This technique was also implemented for quality control and to complement irritation tests.

The development of a relevant FTSm for drug permeation and irritation depends on recreating the skin barrier function to be similar to *in vivo* healthy human skin. The barrier function was characterized using a cytotoxic benchmark known to erode the barrier structure (SDS) and by comparing its permeation profile with accepted models. The open-source FTSm and RHEm presented IC_{50} values within the OECD acceptance limits. Moreover, the tissue damage induced by the cytotoxic benchmark and the resultant disruption of the skin barrier was visualized by passive diffusion of Lucifer yellow. The ability of the produced models to retain the dye in the SC in the absence of passive diffusion showed the integrity of the skin barrier. These findings attest the presence of an intact barrier function in these models, demonstrating their potential to be used as *in vitro* test systems.

The feasibility of using TEER analysis as a multi-purpose tool to evaluate the stages of skin differentiation was assessed by evaluating the impact of topically applied substances on the skin barrier. TEER reflects skin barrier functionality by measuring the overall barrier to ions (Srinivasan et al., 2015). It takes into account the contributions from the SC barrier as well as the viable epidermis by including cell-to-cell tight junctions, which regulate the movement of ions across the paracellular pathway (Groeber et al., 2015; Gorzelanny et al., 2020). In a previous publication, we showed that there is an increase in TEER values in RHEm and FTSm cultured over two weeks at ALI, reflecting progressive SC accumulation and tight junction formation (Zoio et al., 2021a). Here, the TEER was measured on the final day of culture in multiple tissue batches. A mean TEER value of 953 ± 398 $\Omega \cdot cm^2$ was obtained for the FTSm and 11,424 ± 6,033 $\Omega \cdot cm^2$ for the RHEm. These TEER values are consistent with the presence of barrier function integrity.

The high variability of these measurements is not only of biological origin but is also a result of the use of hand-held, chopstick-type electrodes. These electrodes can induce variability between measurements due to variations in the depth and angle of immersion. Furthermore, their geometry cannot deliver a uniform current density across the entire cell culture area. Small changes in temperature during measurements could also have affected the TEER (Srinivasan et al., 2015). For an in-depth discussion related to the limitations of the tetrapolar electrode system for TEER measurements, see (Zoio et al., 2021b). The variability in TEER values can also be a result of differences in tissue thickness and SC architecture. We hypothesize that the lower average TEER values in FTSm compared to RHEm are a result of improper sealing of the scaffold. This phenomenon results in possible channels for fluid and ion transportation and therefore in lower TEER measurements. Taking this into account, TEER values were evaluated independently for each model type.

After studying the developed FTSm and RHEm regarding morphology, viability, and barrier function, preliminary skin irritation tests were performed. In this study, we used the OECD TG 439 to assess the ability of the open-source RHEm and FTSm to correctly classify a test substance as irritating (GHS category 2) or non-irritating (no category). Using the MTT assay, RHEm correctly identified 4/4 substances, and the FTSm correctly identified 3/4 substances. Interestingly, the FTSm determined 1-bromohexane as a non-irritant and RHEm showed viability of 48%, which could be considered as a "borderline" result. Similar results for this substance were also obtained by Mewes et al. (2016) and Jung et al. (2014). In a human patch test, 1-bromohexane was identified as an irritant, but a large variation was observed (Jírová et al., 2010). Mewes et al. (2016) hypothesized that the variability seen in the patch tests was mirrored in the irritation tests using tissue models. The genetic background of the keratinocyte donor, including the ethnic background, could determine the observed variation in the sensitivity to 1-bromohexane. Additional studies are needed to confirm this hypothesis. In general, the FTSm showed higher residual viability when exposed to irritants compared to RHEm (Fig. 6a). This can be explained by the added contribution of the dermal layer. We hypothesize that less test substance can penetrate into the dermal compartment and cause fibroblast death. These studies could also have been affected by limited MTT penetration into the tissue's inner core. Future studies should include the visualization of formazan crystals *in situ* after incubation of the models in MTT.

TEER measurements were performed to complement viability measurements for skin irritation tests. If we consider a threshold of 50% TEER value compared to skin without treatment to identify irritants, all test substances were correctly identified except for isopropanol on FTSm (and with TEER being reduced by 40 ± 10% for RHEm). The significant reduction of the measured TEER values is contradictory to the results of the viability test. This phenomenon was also observed in another study (Groeber et al., 2015). One relevant consideration is that, although the outer epidermal layers are responsible for the major part of the skin barrier function, MTT based assays assess the viability of only the basal cell layer in RHEs (Cotovio et al., 2005). This means that no direct information can be gathered on the effect of a test substance on the outer epidermal layers, such as the SC. The extracellular space of the SC layer is filled with lipids such as free fatty acids, which contribute to the skin barrier (Thakoersing et al., 2013). One hypothesis for the TEER reduction with isopropanol is that the substance dissolves the lipids in the SC, impairing barrier function without affecting viability. In an *in vitro* model,

Cartner et al. (2017) showed that isopropanol causes significant SC perturbation whereas ethanol does not.

Taking into account that a defective barrier can, for example, cause an inflammatory reaction (Seo et al., 2017) as well as sub-irritative effects (stinging, burning, itching), it could be useful to complement viability assays with TEER measurements. However, there is no standard operating procedure to perform TEER measurements on reconstructed skin tissues. Considering the high variability of TEER measurements, it is crucial to optimize the protocol to improve reproducibility. In any case, handheld chopstick electrodes are not suitable to perform standardized TEER measurements, a prerequisite to include this parameter in *in vitro* irritation studies. Alternatively, TEER measurement chambers (e.g., Endohm chamber) containing a pair of concentric electrodes can generate a more uniform current density across the tissue. Moreover, Endohm's fixed geometry increases stability and reproducibility, making this technique more suitable for standardization. The temperature should also be controlled and maintained at 37ºC during the measurements. Acceptability ranges for TEER values should be defined for each skin protocol.

It is a well-known problem that permeation of reconstructed skin models (both FTSm and RHEm) exceeds that of human and pig skin. Schmook et al. (2001) showed that both a FTSm (Graftskin LSE) and a RHEm (Skinethic HRE) were highly permeable for hydrophobic compounds, presenting a 900- and 800-fold higher flux of clotrimazole as compared to human skin, respectively. The group concluded that the available models could not be regarded as useful for *in vitro* permeation studies. Ackermann et al. (2010) reported that the FTSm Phenion® FT presented a weaker barrier than pig skin similar to commercially available RHEm.

Here, the feasibility of using the developed open-source models for permeation assays was evaluated by comparing them with a commercial product that has been tested for a wide range of compounds, i.e., the Strat-M® membrane (Uchida et al., 2015). By comparing the performance of the models with a highly tested commercial product, it was possible to avoid the use of skin tissues from animal or human origin for comparison. The barrier to salicylic acid was comparable between FTSm, RHEm and Strat-M®. For a more hydrophobic compound (clotrimazole), the use of reconstructed skin models resulted in approximately double the flux rate compared to Strat-M®. One possible explanation for the different permeation fluxes is the different effect of propylene glycol on the artificial membrane compared to the cell-based reconstructed models. Propylene glycol was used as a solvent for the topical drugs and as a skin enhancer acting on the intercellular lipid matrix. Carrer et al. (2020) showed that propylene glycol modifies both the epidermis and the dermis by altering the lipidic order of the bilayer structure of the intercellular lipids to a more disordered lipid structure. In this study, the different composition of the Strat-M® and reconstructed skin models could have resulted in a different action of propylene glycol with regard to its skin enhancing abilities. Still, compared to the reconstructed skin models reported by Schmook et al. (2001), the FTSm presents clotrimazole permeation fluxes that are very similar to those of human skin.

The differences between the RHEm and FTSm for hydrocortisone were not expected and probably reflect the different cell batches used for both models and/or the differences in tissue manipulation. During permeation assays, the scaffold membrane of the FTSm is removed from the insert and placed on the 3D printed Franz cell adaptors. These adaptors presented imperfections, and the reproducible sealing could have been compromised. The increased manipulation necessary for the FTSm and imperfect sealing could explain some incoherencies in the results as well as the increased variability. Future experiments should use Franz cell adaptors fabricated using a 3D printer with higher resolution. Still, the FTSm presents a better barrier to hydrocortisone compared to SkinEthic® and Apligraf® (Schmook et al., 2001). Overall, the permeation was comparable between the developed models and commercial Strat-M®, especially regarding the quantities of permeated substances at 24 h.

In the present study, for each test, only one batch of cells was used (N = 1, n = 3). Since primary cells were used, the specific batch and passage number could have affected some of the outcomes and conclusions. Future experiments should expand the present analysis by using more cell batches and by testing a larger array of chemical substances. For irritation tests, the next step should be to test the 20 reference chemicals defined in the OECD performance standards for *in vitro* skin irritation testing. Moreover, the potential of this open-source model should be directly compared to the available commercial models, for example, the EpiSkin® (RHEm) and Phenion® (FTSm).

Importantly, although serum-free culture medium was used for HEKn expansion and differentiation and a human FDM was used instead of animal-derived hydrogels, fetal bovine serum was still included in the current protocol for HDFn expansion. In accordance with the 3R principles, future optimizations to the current protocol should be performed in order to avoid harvesting fetal bovine serum from bovine fetuses. Alternatively, serum-free or xeno-free media should be used in all skin culture steps, including the generation of the dermal compartment.

5 Conclusion

These preliminary studies show the potential of the developed open-source FTSm to be used for skin irritation and permeation studies according to OECD performance standards. This work shows that the innovative approach based on the use of an inert scaffold and a fibroblast-derived matrix results in a well differentiated epidermis with *in vivo*-like barrier function. The preliminary irritation tests performed using MTT lead to a correct classification of all the test substances, except for 1-bromohexane. However, this result may reflect the varying responses to 1-bromohexane seen in *in vivo* models. Complementing the tissue viability assays with TEER measurements resulted in a more comprehensive analysis of skin irritation and opened the possibility to identify sub-irritative effects. During permeation assays, both skin models showed a similar barrier to salicylic acid compared to the commercially produced artificial Strat-M®. For more hydrophobic compounds, the FTSm presented an at least two-

fold permeation flux compared to the Strat-M®. Further studies including more skin batches and a larger array of test substances should be performed. Considering the overall results, the proposed open-source FTSm shows potential for use in safety profiling of topically applied drugs, as well as in the early stages of drug discovery. In the future, the proposed open-source models could help speed up the translation of new candidate therapeutics to the clinic and/or the market and circumvent the current limitations of the available commercial models.

References

Ackermann, K., Lombardi Borgia, S., Korting, H. C. et al. (2010). The Phenion® full-thickness skin model for percutaneous absorption testing. *Skin Pharmacol Physiol 23*, 105-112. doi:10.1159/000265681

Almeida, A., Sarmento, B. and Rodrigues, F. (2017). Insights on in vitro models for safety and toxicity assessment of cosmetic ingredients. *Int J Pharm 519*, 178-185. doi:10.1016/j.ijpharm.2017.01.024

Carrer, V., Alonso, C., Pont, M. et al. (2020). Effect of propylene glycol on the skin penetration of drugs. *Arch Dermatol Res 312*, 337-352. doi:10.1007/s00403-019-02017-5

Cartner, T., Brand, N., Tian, K. et al. (2017). Effect of different alcohols on stratum corneum kallikrein 5 and phospholipase A_2 together with epidermal keratinocytes and skin irritation. *Int J Cosmet Sci 39*, 188-196. doi:10.1111/ics.12364

Cotovio, J., Grandidier, M.-H., Portes, P. et al. (2005). The in vitro acute skin irritation of chemicals: Optimisation of the EPISKIN prediction model within the framework of the ECVAM validation process. *Altern Lab Anim 33*, 329-349. doi:10.1177/026119290503300403

Cross, S. E., Magnusson, B. M., Winckle, G. et al. (2003). Determination of the effect of lipophilicity on the in vitro permeability and tissue reservoir characteristics of topically applied solutes in human skin layers. *J Invest Dermatol 120*, 759-764. doi:10.1046/j.1523-1747.2003.12131.x

Cui, M., Wiraja, C., Chew, S. W. T. et al. (2021). Nanodelivery systems for topical management of skin disorders. *Mol Pharm 18*, 491-505. doi:10.1021/acs.molpharmaceut.0c00154

De Vuyst, E., Charlier, C., Giltaire, S. et al. (2013). Reconstruction of normal and pathological human epidermis on polycarbonate filter. In K. Turksen (ed.), *Epidermal Cells* (191-201). Methods in Molecular Biology (Methods and Protocols), Volume 1195. New York, NY, USA: Springer. doi:10.1007/7651_2013_40

De Wever, B., Kurdykowski, S. and Descargues, P. (2015a). Human skin models for research applications in pharmacology and toxicology: Introducing NativeSkin®, the "missing link" bridging cell culture and/or reconstructed skin models and human clinical testing. *Appl In Vitro Toxicol 1*, 26-32. doi:10.1089/aivt.2014.0010

De Wever, B., Goldberg, A., Eskes, C. et al. (2015b). "Open source" – Based engineered human tissue models: A new gold standard for nonanimal testing through openness, transparency, and collaboration, promoted by the ALEXANDRA association. *Appl In Vitro Toxicol 1*, 5-9. doi:10.1089/aivt.2014.0011

Del Bino, S., Duval, C. and Bernerd, F. (2018). Clinical and biological characterization of skin pigmentation diversity and its consequences on UV impact. *Int J Mol Sci 19*, 2668. doi:10.3390/ijms19092668

Fuggetta, A. (2003). Open source software – An evaluation. *J Syst Softw 66*, 77-90. doi:10.1016/S0164-1212(02)00065-1

Gorzelanny, C., Mess, C., Schneider, S. W. et al. (2020). Skin barriers in dermal drug delivery: Which barriers have to be overcome and how can we measure them? *Pharmaceutics 12*, 684. doi:10.3390/pharmaceutics12070684

Gray, A. C., Sidhu, S. S., Chandrasekera, P. C. et al. (2016). Animal-friendly affinity reagents: Replacing the needless in the haystack. *Trends Biotechnol 34*, 960-969. doi:10.1016/j.tibtech.2016.05.017

Groeber, F., Engelhardt, L., Egger, S. et al. (2015). Impedance spectroscopy for the non-destructive evaluation of in vitro epidermal models. *Pharm Res 32*, 1845-1854. doi:10.1007/s11095-014-1580-3

Jírová, D., Basketter, D., Liebsch, M. et al. (2010). Comparison of human skin irritation patch test data with in vitro skin irritation assays and animal data. *Contact Dermatitis 62*, 109-116. doi:10.1111/j.1600-0536.2009.01640.x

Joffe, R., Plaza, J. A. and Kajoian, A. (2020). Tip chapter: Histology and physiology of the skin. In A. Da Costa (ed.), *Minimally Invasive Aesthetic Procedures: A Guide for Dermatologists and Plastic Surgeons* (179-192). Cham, Switzerland: Springer. doi.org/10.1007/978-3-319-78265-2

Jung, K.-M., Lee, S.-H., Jang, W.-H. et al. (2014). KeraSkin™-VM: A novel reconstructed human epidermis model for skin irritation tests. *Toxicol In Vitro 28*, 742-750. doi:10.1016/j.tiv.2014.02.014

Mewes, K. R., Fischer, A., Zöller, N. N. et al. (2016). Catch-up validation study of an in vitro skin irritation test method based on an open source reconstructed epidermis (phase I). *Toxicol In Vitro 36*, 238-253. doi:10.1016/j.tiv.2016.07.007

Natsuga, K., Watanabe, M., Nishie, W. et al. (2019). Life before and beyond blistering: The role of collagen XVII in epidermal physiology. *Exp Dermatol 28*, 1135-1141. doi:10.1111/exd.13550

Netzlaff, F., Lehr, C. M., Wertz, P. W. et al. (2005). The human epidermis models EpiSkin®, SkinEthic® and EpiDerm®: An evaluation of morphology and their suitability for testing phototoxicity, irritancy, corrosivity, and substance transport. *Eur J Pharm Biopharm 60*, 167-178. doi:10.1016/j.ejpb.2005.03.004

Niehues, H., Bouwstra, J. A., El Ghalbzouri, A. et al. (2018). 3D skin models for 3R research: The potential of 3D reconstructed skin models to study skin barrier function. *Exp Dermatol 27*, 501-511. doi:10.1111/exd.13531

OECD (2021). Test No. 439: In Vitro Skin Irritation: Reconstructed Human Epidermis Test Method. *OECD Guidelines for the Testing of Chemicals, Section 4*. OECD Publishing, Paris. doi:10.1787/9789264242845-en

Perticaroli, S., Yeomans, D. J., Wireko, F. C. et al. (2019). Translating chemometric analysis into physiological insights from in vivo confocal Raman spectroscopy of the human stratum corneum. *Biochim Biophys Acta Biomembr 1861*, 403-409. doi:10.1016/j.bbamem.2018.11.007

Radhakrishnan, S., Nagarajan, S., Bechelany, M. et al. (2020). Collagen based biomaterials for tissue engineering applications: A review. In O. Frank-Kamenetskaya, D. Vlasov, E. G. Panova et al. (eds.), *Processes and Phenomena on the Boundary Between Biogenic and Abiogenic Nature* (3-22). Cham, Switzerland: Springer International Publishing.

Rasmussen, C., Gratz, K., Liebel, F. et al. (2010). The StrataTest® human skin model, a consistent in vitro alternative for toxicological testing. *Toxicol In Vitro 24*, 2021-2029. doi:10.1016/j.tiv.2010.07.027

Redden, R. A. and Doolin, E. J. (2003). Collagen crosslinking and cell density have distinct effects on fibroblast-mediated contraction of collagen gels. *Ski Res Technol 9*, 290-293. doi:10.1034/j.1600-0846.2003.00023.x

Rice, G. and Rompolas, P. (2020). Advances in resolving the heterogeneity and dynamics of keratinocyte differentiation. *Curr Opin Cell Biol 67*, 92-98. doi:10.1016/j.ceb.2020.09.004

Schmook, F. P., Meingassner, J. G. and Billich, A. (2001). Comparison of human skin or epidermis models with human and animal skin in in-vitro percutaneous absorption. *Int J Pharm 215*, 51-56. doi:10.1016/S0378-5173(00)00665-7

Seo, S. R., Lee, S. G., Lee, H. J. et al. (2017). Disrupted skin barrier is associated with burning sensation after topical tacrolimus application in atopic dermatitis. *Acta Derm Venereol 97*, 957-958. doi:10.2340/00015555-2699

Seth, D., Cheldize, K., Brown, D. et al. (2017). Global burden of skin disease: Inequities and innovations. *Curr Dermatol Rep 6*, 204-210. doi:10.1007/s13671-017-0192-7

Srinivasan, B., Kolli, A. R., Esch, M. B. et al. (2015). TEER measurement techniques for in vitro barrier model systems. *J Lab Autom 20*, 107-126. doi:10.1177/2211068214561025

Tadros, A. R., Romanyuk, A., Miller, I. C. et al. (2020). STAR particles for enhanced topical drug and vaccine delivery. *Nat Med 26*, 341-347. doi:10.1038/s41591-020-0787-6

Thakoersing, V. S., van Smeden, J., Mulder, A. A. et al. (2013). Increased presence of monounsaturated fatty acids in the stratum corneum of human skin equivalents. *J Invest Dermatol 133*, 59-67. doi:10.1038/jid.2012.262

Uchida, T., Kadhum, W. R., Kanai, S. et al. (2015). Prediction of skin permeation by chemical compounds using the artificial membrane, Strat-M™. *Eur J Pharm Sci 67*, 113-118. doi:10.1016/j.ejps.2014.11.002

Urciuolo, F., Casale, C., Imparato, G. et al. (2019). Bioengineered skin substitutes: The role of extracellular matrix and vascularization in the healing of deep wounds. *J Clin Med 8*, 2083. doi:10.3390/jcm8122083

van den Broek, L. J., Bergers, L. I. J. C., Reijnders, C. M. A. et al. (2017). Progress and future prospectives in skin-on-chip development with emphasis on the use of different cell types and technical challenges. *Stem Cell Rev Rep 13*, 418-429. doi:10.1007/s12015-017-9737-1

Van Norman, G. A. (2019). Limitations of animal studies for predicting toxicity in clinical trials: Is it time to rethink our current approach? *JACC Basic Transl Sci 4*, 845-854. doi:10.1016/j.jacbts.2019.10.008

Wang, J. X., Fukunaga-Kalabis, M. and Herlyn, M. (2016). Cross-talk in skin: Melanocytes, keratinocytes, stem cells, and melanoma. *J Cell Commun Signal 10*, 191-196. doi:10.1007/s12079-016-0349-3

Yamada, M. and Prow, T. W. (2020). Physical drug delivery enhancement for aged skin, UV damaged skin and skin cancer: Translation and commercialization. *Adv Drug Deliv Rev 153*, 2-17. doi:10.1016/j.addr.2020.04.008

Zoio, P., Ventura, S., Leite, M. et al. (2021a). Pigmented full-thickness human skin model based on a fibroblast-derived matrix for long-term studies. *Tissue Eng Part C Methods 27*, 433-443. doi:10.1089/ten.tec.2021.0069

Zoio, P., Lopes-Ventura , S. and Oliva, A. (2021b). Barrier-on-a-chip with a modular architecture and integrated sensors for real-time measurement of biological barrier function. *Micromachines 12*, 816. doi:10.3390/mi12070816

Zoio, P., Lopes-Ventura, S. and Oliva, A. (2022). Biomimetic full-thickness skin-on-a-chip based on a fibroblast-derived matrix. *Micro 2*, 191-211. doi:10.3390/micro2010013

Zuang, V., Desprez, B., Viegas Barroso, J. et al. (2015). EURL ECVAM Status Report on the Development, Validation and Regulatory Acceptance of Alternative Methods and Approaches. EUR 27474. Luxembourg (Luxembourg): Publications Office of the European Union. JRC97811. doi:10.2788/62058

Conflict of interest

The authors have no conflicts of interest to declare.

Author contributions

P. Zoio developed the skin models, performed the irritation tests, characterization, and the data analysis. P. Zoio wrote the article. S. Ventura contributed to the skin characterization. J. Marto performed the permeation tests and the related data analysis. A. Oliva supervised the project and revised the article.

Data availability statement

The data that support the findings of this study are available from the corresponding author upon reasonable request.

Acknowledgements

iNOVA4Health – UIDB/04462/2020 and UIDP/04462/2020, a program financially supported by Fundação para a Ciência e Tecnologia/Ministério da Educação e Ciência, through national funds and co-funded by FEDER under the PT2020 Partnership Agreement, is acknowledged. P. Zoio acknowledges PD/BD/128164/2016 for the PhD fellowship funded by FCT, Portugal.